# Model for computing superconfiguration temperatures in nonlocal-thermodynamic-equilibrium hot plasmas

J. Bauche and C. Bauche-Arnoult

*Laboratoire Aimé Cotton, Bâtiment 505, Campus d'Orsay, 91405 Orsay, France*

K. B. Fournier

*Lawrence Livermore National Laboratory, P.O. Box 808, Livermore, California 94550, USA*

A model is presented where the level-population densities in quasi-steady-state hot dense plasmas are described by means of large nonrelativistic superconfigurations (SC's), whose configuration populations follow a decreasing-exponential law versus energy (Boltzmann like) for a temperature depending on the SC. Two systems of linear equations are obtained. The first one yields the average-state population densities of the SC's. Using these results, the second system yields the SC temperatures. In this model, a very large number of atomic levels is accounted for in a simple way, thus yielding the configuration populations and, hence, the ionic distribution and average charge. It also yields accurate simulations of the spectra, which are of the essence for emissivity and absorption calculations. It opens a way to time-dependent calculations.

PACS number(s): 52.25.Jm, 52.25.Os, 32.30.Rj

## I. INTRODUCTION

Typical hot-plasma experiments are currently made by interacting lasers with pulse lengths ranging from subpicosecond [1,2] to several nanoseconds [3,4], fast ignitors [5], high-intensity $X$ [6] and $Z$ [7] pinches, hohlraum x-ray drives [8], and coherent x-ray sources [9] with solid and gaseous targets.[1] The plasmas in these experiments form very quickly, reach high electron temperatures, and span a large range of densities. Therefore, for describing the resulting plasma ions, the simple laws of local thermodynamic equilibrium (LTE) are not pertinent. Several non-LTE (NLTE) simulation methods have been proposed, in which the values of the ion population densities (more simply called *populations* in the following) are derived by taking explicitly into account the effects of different atomic processes occurring in the plasma. The results of some of these codes have been presented in a NLTE kinetics workshop [10]. For high-$Z$ plasmas, the discrepancies between the results are very large, and the conclusion is that more work is needed.

Generally, the method used for finding non-LTE level populations is the collisional-radiative model (CRM) [11,12]. It consists in solving a homogeneous system of many linear balance equations. Each equation relates to one atomic $J$ level. The equation represents the equality between the number of atoms that are brought to this level per second and the number of those which leave it. In all hot plasmas, except those of the very light elements, several thousands or millions of levels are needed for obtaining significant physical results. For this reason such systems are not tractable, and some types of global methods have been proposed, in which the individual levels are replaced by large ensembles of levels.

A simple global method consists in defining each *electronic configuration* as one of these ensembles. The average transition rates between configurations are computed, and a CRM system with one equation per configuration is solved [13]. However, more than 10 000 configurations have often to be introduced. For that reason, larger ensembles are preferred—e.g., the *superconfigurations* (SC's), originally defined by Bar-Shalom *et al.* [14]. Among all the published methods, the following two have been the main references for the present work.

In the first method, named AVERROÈS/TRANSPEC [15], each SC is defined as the totality of the configurations possessing the same fixed set of occupation numbers of the atomic shells. For example, $(1)^2(2)^8(3)^5$ represents the 15 electronic configurations with 2, 8, and 5 electrons in the shells $n=1$, 2, and 3, respectively [16]. Average transition rates for the superarrays between the SC's are computed in order to write one CRM equation per SC. Within each SC, the configurations are assumed to be populated according to the electronic temperature $T_e$.

In the second method, named SCROLL [17], the SC's are built from relativistic orbitals. For example, the SC $(1s\,2s\,2p_{1/2}\,2p_{3/2})^4(3p_{1/2}\,3p_{3/2})^2$ contains 69 relativistic configurations. At the beginning, large SC's are defined, average transition rates between the SC's are computed, and the CRM equations are solved for the populations. In subsequent iterations, the SC's are split into smaller and smaller SC's, and the values obtained for their populations are compared with those of the previous step. Iterations are stopped when the changes between two steps are considered to be negligible. At the beginning, the total populations of the relativistic configurations are assumed to obey the statistical law for a temperature $T_z$ proposed by Busquet in the RADIOM model [18]—that is, scaled to give an average ionization state equivalent to an LTE calculation.

Describing the ionic system as a collection of SC's may be insufficient for revealing the spectral details. Indeed, for

---

[1]The references in the preceding sentence are a parochial subset of the available literature and do not represent the broad and dynamic efforts on going in the field of plasma x-ray spectroscopy.

calculating the emissivity and absorption monochromatic coefficients, the transition arrays between electronic configurations are used, e.g., in the unresolved transition arrays (UTA's) formalism [19]. The total population of each configuration must be determined. However, there exists no proof that, within each SC, the populations of the configurations follow a temperature law for either $T_e$ or $T_z$. We propose another type of model, where within each (nonrelativistic) SC the populations of the configurations obey a temperature law for an *effective temperature* $T(SC)$ specific to that SC. Each configuration is represented by its average energy, with the assumption that its $JM$ states are degenerate. The CRM system is built with one equation per SC. Its numerical coefficients are combinations of configuration-to-configuration transition rates. It happens that it is possible to split the initial system into two systems of the same size, one related to the SC populations and the other one to the SC temperatures. From these results, one deduces in a very simple way the configuration populations. It is assumed that, *within each configuration*, the quantum *states* $\alpha J M_J$ of all the $\alpha J$ energy levels (where $\alpha$ denotes the relevant coupling scheme) are equally populated.

This model is essentially nonrelativistic (see Sec. V E). The LTE laws are not applied, except the Maxwell-distribution law for the free-electron velocities, whose characteristic time is much shorter than those of the atomic processes. The time-consuming splitting/iteration procedures and the use of partition functions are avoided. Well-balanced sets of SC's are employed, and convergence is reached when the number of SC's introduced is large enough. Let this number be 200 instead of 100; the increase in the complexity of the calculations is moderate.

In Sec. II, the concept of effective temperatures is supported by the correlations, which are explained in Sec. III. The relevant equations of the model are derived in Sec. IV. A discussion and conclusion are given in Secs. V and VI.

## II. TEMPERATURE LAWS

The concept of effective temperatures specific to electronic configurations in an atomic plasma has first appeared in the results of tensor-operator calculations [20,21] of spontaneous emission in the Fe V spectrum. More precisely, if the level populations of an upper configuration $C' = n\ell^N n'\ell'$ (with $|\ell - \ell'| = 1$) obey the Boltzmann decreasing-exponential law for some *configuration temperature* $T_{C'}$, the radiative transfers to the levels of $C = n\ell^{N+1}$ enforce the same type of law for another temperature $T_C$ [22].

The above derivation can be extended from spontaneous emission to the other seven important *monoelectronic* atomic processes: i.e., radiative absorption, collisional excitation and deexcitation, photoionization and radiative recombination, collisional ionization, and three-body recombination. This extension is evident for the first process, which is the inverse of radiative emission. In general, it can be demonstrated rigorously for the processes that involve free electrons, in the assumption that the radial quantity with a given name has the same value for all the levels of a configuration. Thus, it is not surprising that it holds fairly well for colli-
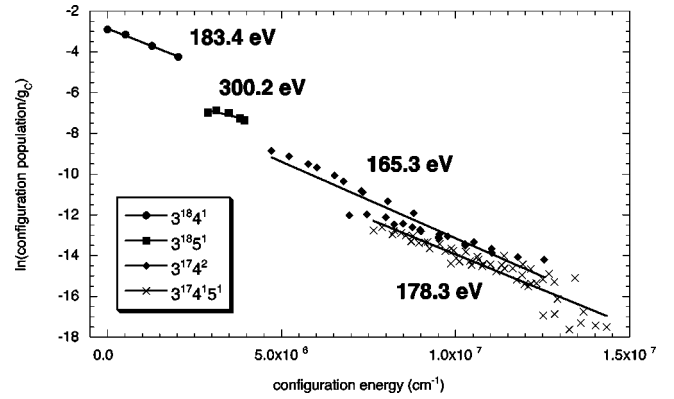


FIG. 1. Evidence for superconfiguration temperatures in Xe XXVI (Cu like). The level populations are determined by means of a level-by-level CRM calculation. They are summed into configuration populations. The average populations are deduced by dividing by the degenaracies. The logarithms of these average populations (circles, squares, diamonds, crosses) are fitted by the least-squares method to four segments, whose slopes are equal to the inverse SC temperatures. For these fits, the values of Pearson's $r$ coefficient are equal to 0.996, 0.861, 0.988, and 0.965, respectively.

sional excitation and deexcitation, in agreement with the results of Van Regemorter [23].

When a quasi-steady-state CRM calculation is computed for a large number of levels, the populations of the levels of each configuration $C$ tend to obey a temperature law for a specific $T_C$ value [24]. This has been checked numerically in three isoelectronic series of ions, $_{26}$Fe IV-V-VI, $_{36}$Kr XIV-XV-XVI, and $_{42}$Mo XX-XXI-XXII, for the same set of configurations [25]. This set contains 27 configurations, with 4668 levels. Several electronic densities are assumed. Three through eight atomic processes have been introduced, for which the transition rates have been computed by means of the HULLAC code [26]. The temperature of each configuration is determined by fitting the values found for the populations of its $JM$ states (i.e., the $J$-level populations divided by $2J + 1$) to a decreasing-exponential law. The uncertainties found in the fitting process are small. For the lowest electronic densities computed ($10^{14}$ or $10^{16}$ cm$^{-3}$), the obtained temperatures are about 3 or 4 times smaller than $T_e$, which means that the system is far from LTE [25].

Proving the existence of SC temperatures is more difficult, due to the complexity of the SC's [27]. Indeed, no analytic derivation of SC temperatures has yet been found by means of Racah algebra, even for spontaneous emission. However, (i) there exist strong similarities between the transitions between the configurations and those between SC's, and (ii) the existence of specific temperatures within the configurations can be explained analytically [22] and demonstrated numerically [25]. *In fine*, only approximate relations can be used for writing the equations that yield the *superconfiguration temperatures* in a hot plasma [28] (see Sec. III). In the following, they are called *correlations*.

Fortunately, it is possible to demonstrate numerically, by means of an ordinary collisional-radiative computation, that the populations of the $JM$ states of some simple SC's tend to obey a temperature law. An example is presented in Fig. 1,

for the case of four SC's $((3)^{18}(4)^1,(3)^{18}(5)^1,(3)^{17}(4)^2,(3)^{17}(4)^1(5)^1)$ in the Xe XXVI (Cu-like) ion and three SC's $((3)^{18},(3)^{17}(4)^1,(3)^{17}(5)^1)$ in the Xe XXVII (Ni-like) ion, which contain altogether 4567 Cu-like and 249 Ni-like levels. Eight major processes are accounted for: namely, spontaneous emission, collisional excitation and deexcitation, collisional ionization and three-body recombination, autoionization and resonant capture, and radiative recombination. The input data are the electronic density $n_e = 1.2 \times 10^{20}$ cm$^{-3}$ and temperature $T_e = 450$ eV. The $n_e$ value is that of an optically thin plasma, which justifies that radiative absorption and photoionization are not considered. Moreover, it has been found experimentally that the Cu- and Ni-like ions are abundant for these values of $n_e$ and $T_e$ [3]. First, all these 4816 levels are entered in a level-by-level CRM calculation and steady-state level populations are found. Second, (i) summing the populations found for the Cu-like levels (the most numerous in the calculated list) yields the populations of the corresponding 91 configurations, (ii) the population of each configuration is divided by the degeneracy for obtaining the average-state population, (iii) the logarithms of these average-state populations are plotted versus the configuration-average energies, and (iv) the points of this plot are fitted by least squares to four straight lines, which correspond to the four relevant SC's.

The values deduced for the four SC temperatures are presented in Fig. 1. Based on the linear variation of the logarithms of the average-state populations, the concept of SC temperatures, different from $T_e$, appears to be quite relevant. It is noteworthy that the SC $(3)^{17}(4)^2$ looks like it contains two sets of configurations with different temperatures. However, the straight line that is drawn has been obtained by means of a degeneracy-weighted rms calculation. The fact that it nearly coincides with one of the two sets, with an excellent Pearson's $r$ coefficient, means that the other set mainly contains configurations with a lower degeneracy, so that the global description of the populations is satisfactory.

### III. CORRELATIONS BETWEEN TWO SC's

In the place of exact relations, it is possible to find *correlations* between two SC's that are linked by some atomic process (or within one SC, where this process occurs). In the present work, this word simply means *approximate linear relations*. Their coefficients can be obtained by solving through the least-squares method systems of linear equations.

#### A. Typical example: Radiative emission

Radiative emission is the simplest process for demonstrating the existence and the calculation of correlations between SC's. The basic equation is that for the total strength $S(C' \rightarrow C)$ of the electric-dipolar transition array between configurations $C$ and $C'$:

$$S(n\ell^N n'\ell'^{N'+1} n''\ell''^{N''} \cdots \rightarrow n\ell^{N+1} n'\ell'^{N'} n''\ell''^{N''} \cdots)$$

$$= 2\ell_> P(n\ell,n'\ell')^2 \binom{4\ell+1}{N}\binom{4\ell'+1}{N'}\binom{4\ell''+2}{N''}\cdots,$$

$$\tag{1}$$

where $P(n\ell,n'\ell')$ is the radial integral $\int_0^\infty u_{n\ell}(r) r u_{n'\ell'}(r) r^2 dr$ for electric-dipolar radiative transitions, and $\ell_>$ is the larger of the two orbital quantum numbers $\ell$ and $\ell'$, and where there may occur more than one *spectator* open subshell like $n''\ell''^{N''}$ [29]. This formula is interesting because (i) the selection rule $|\ell-\ell'|=1$ strongly reduces the number of arrays, (ii) the values of the $P(n\ell,n'\ell')$ radial integrals can be assumed as independent of the considered array, and (iii) for fixed values of $n$ and $n'$, with $n < n'$, the largest integral is, by far, that with $\ell = n - 1$ and $\ell' = n$.

#### 1. First correlation: Correlation between the configuration energies

In general, in the superarray $(SC' \rightarrow SC) = ((n)^N (n')^{N'+1} \rightarrow (n)^{N+1}(n')^{N'})$, the higher- (lower-) energy configurations of $SC'$ deexcite preferably towards the higher- (lower-) energy configurations of $SC$. Indeed, in each transition array, the lower and upper configurations only differ by one orbital. The (often) numerous spectator orbitals are unchanged. When most of them are high-energy (low-energy) orbitals, the energies of both configurations range among the highest (lowest) in their $SC$. This correlation has also been called a propensity law, when applied to the case of energy levels in the transition array between configurations (p. 337 in Ref. [30]). It is characterized by a coefficient denoted $\rho(SC' \rightarrow SC)$, which is calculated by means of a strength-weighted root-mean-squares equation, which expresses the approximate proportionality between $\Delta E(C_j') = E(C_j') - E_{av}(SC')$ and $\Delta E(C_i) = E(C_i) - E_{av}(SC)$, where $i$ and $j$ refer to configurations of $SC$ and $SC'$, respectively, $E(C_i)$ and $E(C_j')$ are the configuration energies, and $E_{av}(SC)$ and $E_{av}(SC')$ are the weighted average energies of the configurations of $SC$ and $SC'$, respectively. The $\rho$ coefficient obeys the equation

$$\sum_{i,j} S(C_j' \rightarrow C_i) \Delta E(C_i) \Delta E(C_j')$$

$$= \rho(SC' \rightarrow SC) \sum_{i,j} S(C_j' \rightarrow C_i) \Delta E(C_i)^2. \quad (2)$$

In Eq. (2), $S(C_j' \rightarrow C_i)$ is the strength of the $C_j' \rightarrow C_i$ array. It is defined (like for all processes) as the product $R(C_j' \rightarrow C_i) g(C_j')$ of the transition *rate* $R$ by the degeneracy $g$ of the initial configuration.
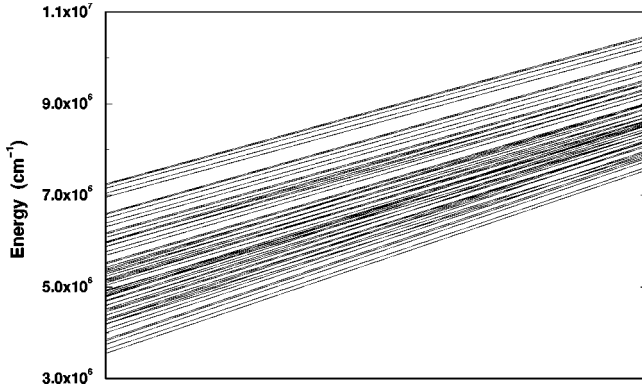
FIG. 2. Correlation between the configuration energies in the $(3)^4(5)^1$-$(3)^3(5)^2$ superarray of Ge XVIII. Each point in the vertical scale on the left represents the energy of a configuration of $(3)^4(5)^1$. It is linked by a straight line to a point on the right, whose ordinate is the weighted average energy of all the configurations of $(3)^3(5)^2$, each weight being the relevant electric-dipolar strength. It can be seen that the higher (lower) configurations of $(3)^3(5)^2$ deexcite preferably towards the higher (lower) configurations of $(3)^4(5)^1$.

This correlation is exemplified in Fig. 2 for a spontaneous-emission array. In this plot, each segment links the point representing a configuration $C_i$ to that representing the strength-weighted average energy of the $C_j'$ configurations. The fact that most of these segments do not cross is the correlation phenomenon.

### 2. Second correlation: Correlation between the array strengths and the configuration energies

In each $SC' \rightarrow SC$ superarray, the second correlation relates the energy of each configuration of $SC$ to the total strength of the transition arrays that are linked to it. It reads

$$\frac{\Sigma_j S(C_j' \rightarrow C_i)}{g(C_i)} = \alpha(SC' \rightarrow SC) + \beta(SC' \rightarrow SC)\Delta E(C_i), \tag{3}$$

with the same notations as in Eq. (2), and where $g(C_i)$ is the degeneracy of configuration $i$. It can also be written for $SC'$, for the same atomic process, in the form

$$\frac{\Sigma_i S(C_j' \rightarrow C_i)}{g(C_j')} = \gamma(SC' \rightarrow SC) + \delta(SC' \rightarrow SC)\Delta E(C_j'). \tag{4}$$

For this correlation, the pertinent graphs are such that the left-hand parts of Eqs. (3) and (4) are plotted versus the energies $\Delta E(C_i)$ and $\Delta E(C_j')$, respectively. In general, the corresponding $\alpha(SC' \rightarrow SC)$, $\beta(SC' \rightarrow SC)$, $\gamma(SC' \rightarrow SC)$, and $\delta(SC' \rightarrow SC)$ coefficients are deduced from such plots through least-squares fits to the linear expansions in Eqs. (3) and (4). This correlation can be derived analytically in some simple cases [28]. It is generally less well obeyed than the first one.

### B. Generalization to the other atomic processes

The validity of the first correlation [Eq. (2)] can be extended from spontaneous emission to all the other seven important *monoelectronic* atomic processes. Indeed, this correlation is essentially based on the fact that only *one* electron changes in the process, whereas the same spectator electrons are responsible for the bulk of the energies of both configurations in a transition array. Four numerical examples are presented in Fig. 3, for four different processes: namely, spontaneous emission, collisional excitation, collisional ionization, and autoionization. Actually, autoionization is a *dielectronic* process. On the average, the first correlation is less well obeyed than for the monoelectronic processes, because it is based on the fact that only *two* electrons change.

The validity of the second correlation [Eqs. (3) and (4)] can be extended to collisional excitation and deexcitation, whose rates have large values only for optically allowed transitions [23]. It can also be extended to photoionization and radiative recombination, for which it is known that the dominant radial parameters relate to the same pairs of orbitals as those for radiative emission. Four numerical examples are presented in Fig. 4, for the same four processes as in Fig. 3.

## IV. COLLISIONAL-RADIATIVE EQUATIONS

### A. General transfer equation

The quantity that represents the transfer of atoms per unit time from all the configurations of the ions to some configuration $C_i$ of superconfiguration $SC$ reads $\Sigma_{P,SC',j}R(P,C_j' \rightarrow C_i)N(C_j')$. In this sum, $N(C_j')$ is the population of configuration $C_j'$, $P$ is an atomic process, and $R(P, C_j' \rightarrow C_i)$ is a transfer rate from $C_j'$ to $C_i$. The temperature law in $SC'$ is written in the form

$$N(C_j') = g(C_j')n(SC')\exp\left(-\frac{\Delta E(C_j')}{kT(SC')}\right), \tag{5}$$

where $n(SC')$ is defined as the *average-state* population of $C_j'$. The quantity $n(SC')$ can also be written as the total population of $SC'$ divided by the partition function of $SC'$ for temperature $T(SC')$. Thus, the total transfer of atoms towards $C_i$ reads

$$\left[\frac{dN(C_i)}{dt}\right]_{\text{in}} = \sum_{P,SC',j} R(P,C_j' \rightarrow C_i)g(C_j')n(SC')$$
$$\times \exp\left(-\frac{\Delta E(C_j')}{kT(SC')}\right). \tag{6}$$

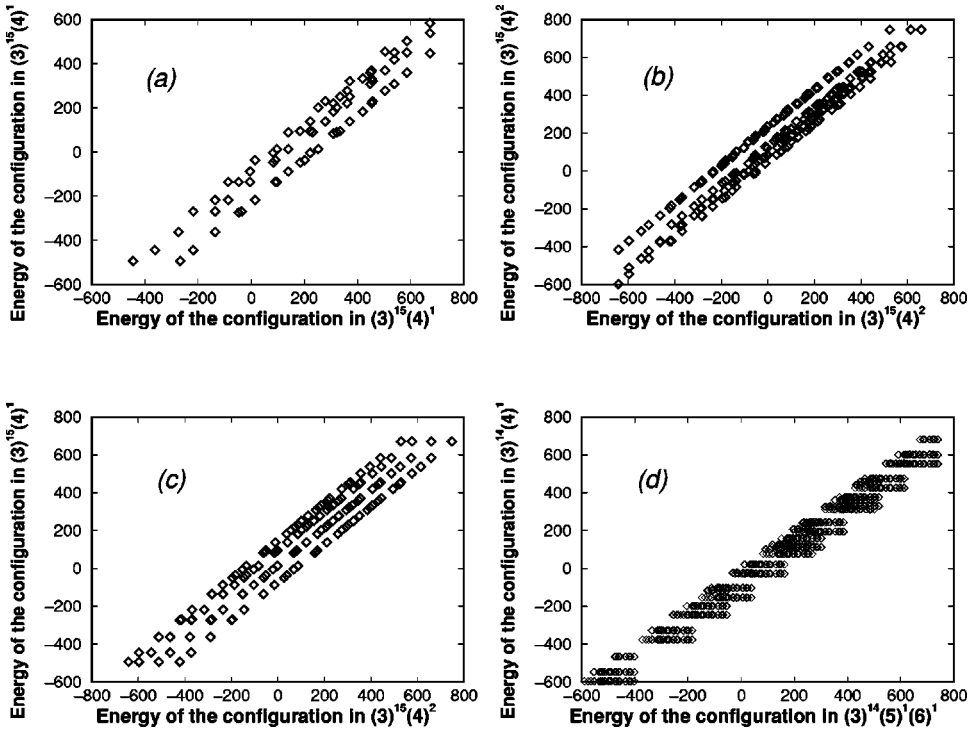By definition, the product $R(P,C_j' \rightarrow C_i)g(C_j')$ is the total

FIG. 3. Correlations between the configuration energies of two SC's. In each plot, the abscissa and the ordinate of each point are the energies of two configurations linked by an atomic process, respectively. (a) Xe XXIX, spontaneous emission within $(3)^{15}(4)^1$. (b) Xe XXVIII, collisional excitation within $(3)^{15}(4)^2$. (c) Xe XXVIII and Xe XXIX, collisional ionization from $(3)^{15}(4)^2$ to $(3)^{15}(4)^1$. (d) Xe XXIX and Xe XXX, autoionization from $(3)^{14}(5)^1(6)^1$ to $(3)^{14}(4)^1$. All energies are in eV.

strength $S(P,C'_j \to C_i)$ of the transitions from $C'_j$ to $C_i$ through the $P$ process. The sum over $j$ also includes the levels that belong to $SC$, but not to $C_i$.

The correlation laws introduced in Sec. III are now taken into account. Through the first one, the energy in Eq. (6) can be replaced by the product $\rho(P,SC' \to SC)\Delta E(C_i)$. Through the second one, the sum $\Sigma_j R(P,C'_j \to C_i)g(C'_j)$ is replaced by $g(C_i)[\alpha(P,SC' \to SC) + \beta(P,SC' \to SC)\Delta E(C_i)]$. In this way, the $C'_j$ configuration disappears from the formula for the transfer:

$$\left[\frac{dN(C_i)}{dt}\right]_{\text{in}} = g(C_i)\sum_{P,SC'} n(SC')[\alpha(P,SC' \to SC) + \beta(P,SC' \to SC)\Delta E(C_i)]\exp\left(-\frac{\rho(P,SC' \to SC)\Delta E(C_i)}{kT(SC')}\right). \quad (7)$$

In the final equation for $dN(C_i)/dt$, one also includes the contributions of the processes which transfer atoms *from* $C_i$ to all the other configurations of the system. For that purpose, Eqs. (4) and (5) are applied, yielding

$$\frac{dN(C_i)}{dt} = g(C_i)\sum_{P,SC'} n(SC')[\alpha(P,SC' \to SC) + \beta(P,SC' \to SC)\Delta E(C_i)]\exp\left(-\frac{\rho(P,SC' \to SC)\Delta E(C_i)}{kT(SC')}\right)$$

$$- g(C_i)n(SC)\exp\left(-\frac{\Delta E(C_i)}{kT(SC)}\right)\sum_{P,SC'}[\gamma(P,SC \to SC') + \delta(P,SC \to SC')\Delta E(C_i)]. \quad (8)$$

We call Eq. (8) the *master equation* of the model. In the sums, $SC'$ is not necessarily different from $SC$, because summing over $P$ ought to include the processes which are responsible for the transfers between the configurations within $SC$.

### B. Linearization of the collisional-radiative equations

Equation (8) is a balance equation. In the quasi-steady-state approximation, $dN(C_i)/dt$ is equal to zero. One is left with a set of nonlinear coupled equations (one per superconfiguration), where the unknown quantities are the average-state populations $n(SC')$ and the inverse temperatures $1/T(SC')$ of all the SC's. It is essential to linearize these equations with respect to the latter type of unknown quantities.

First, one can divide the first sum in Eq. (8) by the second sum, which gives
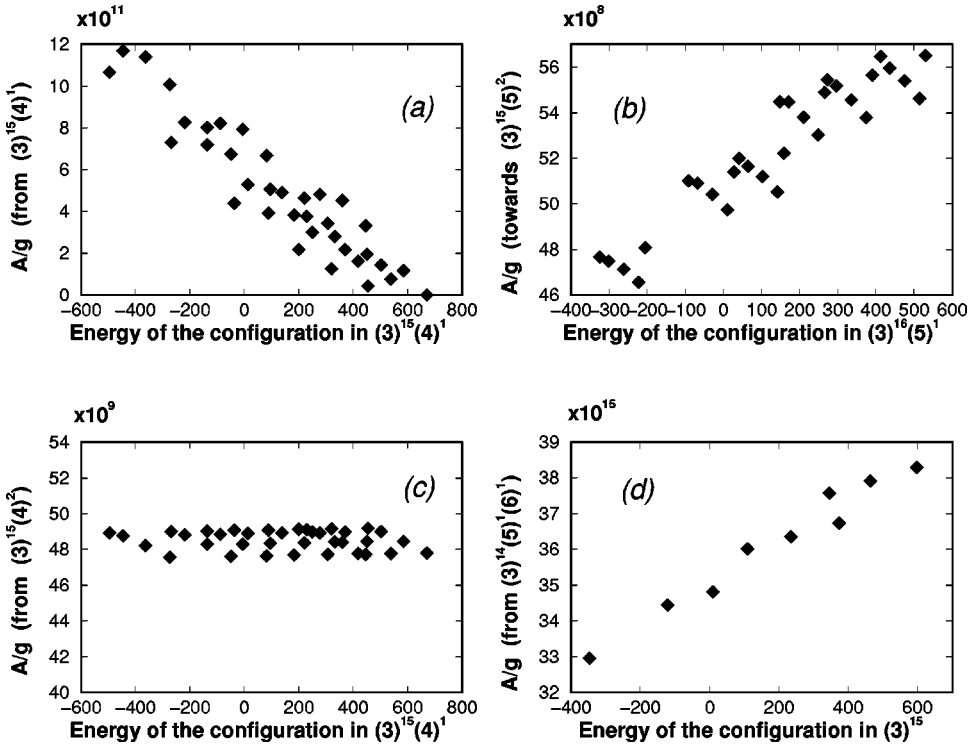
FIG. 4. Correlations between array strengths and configuration energies. In each plot, the abscissa of each point is the energy of a configuration in some SC, and its ordinate is the sum of the strengths of the transitions which are linked to that configuration by some atomic process, divided by its degeneracy. (a) Xe XXIX, spontaneous emission within $(3)^{15}(4)^1$. (b) Xe XXVIII, collisional excitation from $(3)^{16}(5)^1$ to $(3)^{15}(5)^2$. (c) Xe XXIX and Xe XXVIII, collisional ionization from $(3)^{15}(4)^2$ to $(3)^{15}(4)^1$. (d) Xe XXIX and Xe XXX, autoionization from $(3)^{14}(4)^1(5)^1$ to $(3)^{15}$. Ordinates are in atomic units and abscissas are in eV.

$$\sum_{P,SC'} n(SC') \frac{\alpha(P,SC'\to SC)+\beta(P,SC'\to SC)\Delta E(C_i)}{\Sigma_{P,SC'}[\gamma(P,SC\to SC')+\delta(P,SC\to SC')\Delta E(C_i)]} \exp\left(-\frac{\rho(P,SC'\to SC)\Delta E(C_i)}{kT(SC')}\right)$$

$$=n(SC)\exp\left(-\frac{\Delta E(C_i)}{kT(SC)}\right). \tag{9}$$

The fraction in the first line of Eq. (9) is not a linear function of $\Delta E(C_i)$. But it can be approximated by the linear expansion

$$q(P,SC'\to SC)+r(P,SC'\to SC)\Delta E(C_i),$$

where the coefficients $q$ and $r$ are determined as is shown in the Appendix.

Second, after dividing the exponential function in the first term of Eq. (9) by that in the second term, one obtains

$$\sum_{P,SC'} n(SC')[q(P,SC'\to SC)+r(P,SC'\to SC)\Delta E(C_i)]\exp\left(-\frac{\rho(P,SC'\to SC)\Delta E(C_i)}{kT(SC')}+\frac{\Delta E(C_i)}{kT(SC)}\right)=n(SC). \tag{10}$$

Most often, the $\rho$ factors do not differ much from 1 (see Sec. V D). Therefore, for expanding safely the exponential function as a linear function of $\Delta E(C_i)$, it is not necessary that $\Delta E(C_i)$ be much smaller than $kT(SC)$ and $kT(SC')$. It is only necessary that all the temperatures do not differ too much one from the other, within each pair of neighboring ions.

### C. Splitting of the collisional-radiative system of equations

Actually, Eq. (10) is valid for all the configurations of the ions in the plasma. By making all the $\Delta E(C_i)$ quantities

equal to zero, one obtains a system of homogeneous linear equations for the average-state populations. The equation for superconfiguration $SC$ reads

$$\sum_{P,SC'} n(SC')q(P,SC'\to SC)=n(SC). \tag{11}$$

Subtracting Eq. (11) from Eq. (10), expanding linearly the exponential function, dropping terms in $\Delta E(C_i)^2$ (this approximation is discussed in Sec. V D), and dividing the whole equation by $\Delta E(C_i)$, one obtains a system of inho-

mogeneous linear equations for the inverses of the *SC* temperatures. The equation for superconfiguration *SC* reads

$$
\sum_{P,SC'} n(SC') \left[ q(P,SC' \to SC) \left( \frac{\rho(P,SC' \to SC)}{kT(SC')} \right. \right.
$$
$$
\left. \left. - \frac{1}{kT(SC)} \right) - r(P,SC' \to SC) \right] = 0. \tag{12}
$$

The computation runs as follows. First, the system of equations (11) for the average-state populations of the SC's is solved. Second, its numerical solutions are implemented into the system of equations (12), which can be solved for the inverse temperatures of the SC's.

## V. DISCUSSION

### A. Numerical application

Much information has already been gained from the first numerical application of the present model [31]. The case studied is that of an experimentally well-characterized xenon plasma, for the electronic density $1.3 \times 10^{20}$ cm$^{-3}$ and temperature 415 eV [3]. The relevant ions range from Xe XXIV to Xe XXXI. In each ion, 13 or 14 SC's are selected. They constitute two sets. The first set of SC's is $KL(3)^N$, $KL(3)^{N-1}(4,5,6,7,8)^1$, $KL(3)^{N-2}(4)^2$, $KL(3)^{N-2}(4)^1(5,6,7,8)^1$, and $KL(3)^{N-2}(5,6)^2$, in the notation for the SC's, with $N=14$–18. The second set reads $KLM(4)^{N'}$, $KLM(4)^{N'-1}(5,6,7,8)^1$, $KL(3)^{17}(4)^{N'+1}$, $KL(3)^{17}(4)^{N'}(5,6,7,8)^1$, and $KL(3)^{17}(4)^{N'-1}(5,6)^2$, with $N'=1$–3. Here $K$, $L$, and $M$ represent the complete shells $n=1$, 2, and 3, respectively. For example, the SC's considered for Xe XXVIII and the numbers of their configurations are listed in the first two columns of Table I. The $n(SC)$ and $T(SC)$ values have been determined numerically. The populations of all the configurations, hence, those of the SC's, have been obtained by means of Eq. (5).

The obtained ionic distribution is very close to that published previously [3]. For the comparison with the experimental spectrum, the fact that the model yields the configuration populations is essential, because these populations can be entered into the formalism of unresolved transition arrays—i.e., in the form of UTA's or spin-orbit-split arrays (SOSA's) [19].

### B. Selection of the superconfigurations

In the model, the atomic levels are gathered into SC's, which are, actually, pairs of Layzer complexes [16]. This choice offers several advantages. First, the number of SC's is relatively small, because they have large degeneracies and because they are nonrelativistic (see Sec. V E below). Second, they possess some correlation properties, which have been foreseen in special cases and which are crucial for developing the model. Third, the sets of SC's chosen for the various ions resemble each other very much, because they

TABLE I. Superconfigurations introduced for Xe XXVIII (Co-like).

| Superconfiguration | No. conf. | $kT(SC)$ (eV) | Relative population | Incoming flux (s$^{-1}$) |
|---|---|---|---|---|
| $(3)^{17}$ | 3 | 175 | $8.95 \times 10^{-1}$ | $1.72 \times 10^{11}$ |
| $(3)^{16}(4)^1$ | 24 | 189 | $7.81 \times 10^{-2}$ | $6.52 \times 10^{10}$ |
| $(3)^{16}(5)^1$ | 30 | 175 | $6.22 \times 10^{-3}$ | $9.66 \times 10^{9}$ |
| $(3)^{16}(6)^1$ | 36 | 108 | $1.81 \times 10^{-3}$ | $3.72 \times 10^{9}$ |
| $(3)^{16}(7)^1$ | 42 | 176 | $1.45 \times 10^{-4}$ | $2.65 \times 10^{9}$ |
| $(3)^{16}(8)^1$ | 48 | 220 | $1.17 \times 10^{-4}$ | $1.60 \times 10^{9}$ |
| $(3)^{15}(4)^2$ | 90 | 168 | $2.20 \times 10^{-3}$ | $2.66 \times 10^{10}$ |
| $(3)^{15}(4)^1(5)^1$ | 180 | 169 | $2.30 \times 10^{-3}$ | $1.21 \times 10^{10}$ |
| $(3)^{15}(4)^1(6)^1$ | 216 | 126 | $1.52 \times 10^{-3}$ | $4.78 \times 10^{9}$ |
| $(3)^{15}(4)^1(7)^1$ | 252 | 118 | $3.21 \times 10^{-4}$ | $2.61 \times 10^{9}$ |
| $(3)^{15}(4)^1(8)^1$ | 288 | 123 | $2.11 \times 10^{-4}$ | $1.48 \times 10^{9}$ |
| $(3)^{15}(5)^2$ | 135 | 144 | $1.90 \times 10^{-4}$ | $1.07 \times 10^{9}$ |
| $(3)^{15}(5)^1(6)^1$ | 270 | 139 | $6.70 \times 10^{-5}$ | $8.32 \times 10^{8}$ |
| $(3)^{15}(6)^2$ | 189 | 124 | $1.58 \times 10^{-5}$ | $1.56 \times 10^{8}$ |

only differ by the total numbers of electrons (see Sec. V A above). In this way, it is ensured that the totality of the sets is well balanced.

The number of SC's that ought to be considered for solving a given physical situation remains an open problem. We consider that it suffices to choose enough well-balanced sets of SC's for neighboring ions, like those defined in Sec. V A. This avoids resorting to the use of partition functions. The partition function is the Saha-Boltzmann population of a given SC in the considered space of SC's for a given temperature, which may or may not be the temperature of the free electrons that drive the system [18]. In order to converge to a truly non-LTE set of SC populations, one must iteratively split the considered SC's, recompute the partition functions, and then recompute the resulting SC populations [17]. Our method avoids starting from a Saha-Boltzmann description of SC populations at some (adapted) temperature and avoids iteratively generating rates and resolving the master equation.

### C. Relevance of the high-lying SC's

It is interesting to discuss the necessity of introducing the high-lying SC's in numerical applications of the model. For that purpose, one can compare the relative contributions of the SC's (i) to the total populations of the ions and (ii) to the transfers between the SC's. This comparison can be seen in Table I for the 14 SC's of the Xe XXVIII ion (Co-like). For each SC, the incoming flux (in the far-right column) is defined as the total number of the atoms which are brought, per unit time, summed over the different processes, either from the upper or from the lower Co-like SC's or from the SC's of the neighboring Fe- and Ni-like ions. The comparison is most striking for the lowest $[(3)^{17}]$ and the 12th $[(3)^{15}(5)^2]$ SC's. Whereas the 12th is 4500 times less populated than the lowest, its incoming flux is only 160 times smaller. The incoming fluxes are also very large for $(3)^{15}(4)^2$ and $(3)^{15}(4)(5)$. It can be checked that this is due to very active

TABLE II. Total flux per process (s$^{-1}$).

| | |
|---|---|
| Spontaneous emission | $7.92 \times 10^{11}$ |
| Collisional excitation | $3.18 \times 10^{11}$ |
| Collisional deexcitation | $4.87 \times 10^{11}$ |
| Collisional ionization | $5.52 \times 10^{9}$ |
| Radiative recombination | $1.52 \times 10^{9}$ |
| Three-body recombination | $3.70 \times 10^{7}$ |
| Autoionization | $4.12 \times 10^{11}$ |
| Resonant capture | $4.16 \times 10^{11}$ |

autoionization and resonant-capture channels, which happen to predominate by one order of magnitude over the spontaneous-emission process. It can be concluded that the highest SC's definitely participate in the dynamical equilibrium of the level populations, although they contribute very little to the emitted spectrum.

For the relative importance of the various processes, another kind of comparison is presented in Table II. For each process, the total flux is the sum of the incoming fluxes to all the SC's. In this way, it appears that autoionization and resonant capture have fluxes nearly equal to the largest three: namely, those of spontaneous emission and collisional excitation and deexcitation. The importance of these dielectronic processes has already been stressed [32,4]. Here, it has also been found that, if the autoionization and resonant-capture processes are discarded from the calculations, the average charge increases by more than four charges. Moreover, it has been seen that about 30% of the total autoionization flux goes to SC's that are not the lowest in their respective ions.

### D. Validation of the linearization procedures

In addition to the initial basic assumption of the temperature law, two important approximations ought to be validated. First, the linear correlations often correspond to much less convincing plots than those of Figs. 3 and 4. However, it has been found, in the example of the xenon plasma, that the processes with the best correlation plots correspond to the largest transfers of atoms between the SC's (the sizes of the transfers by the different atomic processes are compared in Sec. V C).

Second, the linearization of some exponential functions is questionable. The most important is that which yields Eq. (12). Is the quantity

$$ x = [-\rho(P, SC' \rightarrow SC)/kT(SC') + 1/kT(SC)]\Delta E(C_1) $$

always small enough (in absolute value) for the expansion $(1+x)$ to be a good approximation of the exponential function $e^x$? It was possible to test this approximation in the case of xenon. The value of $x$ has been computed for all the 2298 $SC' \rightarrow SC$ superarrays encountered in that case. It has been

found that the value of the (positive) relative difference ($e^x - 1 - x)/e^x$ is smaller than 0.18 in 74% of the superarrays. This is a favorable test. It is significant, although it is made *a posteriori*.

### E. Relativistic effects

The transition rates used in the present work are calculated between nonrelativistic configurations. However, the gross relativistic effects are taken into account in the sense that the energy Slater integrals and the transition rates are computed in the Pauli-Breit approximation. The *J*-dependent relativistic effects can be neglected for the determination of populations and temperatures. For example, the spin-orbit effects are not expected to have any noticeable importance in the population regime, because the collisional transition rates are made of off-diagonal elements of $G$, the electrostatic-repulsion operator [13].

However, after the populations have been obtained, *J*-dependent relativistic effects may be important for the final calculations of emissivity and absorption. Indeed, they often result in the breaking of transition arrays (UTA's) into spin-orbit split arrays (SOSA's), in which the electric-dipolar transition integrals are *J* dependent.

### VI. SUMMARY AND CONCLUSION

In conclusion, the method of superconfiguration temperatures is a type of collisional-radiative model where dozens of thousands of electronic configurations can be accounted for by solving small-size systems of linear equations. The operations run as follows.

(i) The coefficients for the linear equations are deduced from those for the transition rates between configurations, calculated through existing codes.

(ii) The system of equations for the average-state populations of the SC's is solved.

(iii) Using these populations, the system of equations for the temperatures of the SC's is solved.

(iv) The populations of the configurations are deduced, using Eq. (5), and they are added for each of the ions. This yields the ionic balance of the plasma and the $Z^*$ value.

(v) The spectra of the different ions are calculated in detail, using the UTA and SOSA formalisms. They are essential data for emissivity and absorption calculations.

The model has been applied successfully to the case of a xenon plasma with density $n_e = 10^{20}$ cm$^{-3}$ and temperature $T_e = 450$ eV. The calculated SC's represent about $66 \times 10^6$ levels. Most of the obtained SC temperatures lie in the range 100–200 eV, which is the signature of plasma conditions far from LTE.

Another temperature law has been observed. The average-state populations computed for Xe XXIV–XXXI nearly obey a decreasing-exponential law versus energy. Thus, one can say that there appears a kind of *ionic excitation temperature*, specific to each ion [31].

Two major processes have not yet been introduced in numerical studies: namely, photoionization and radiative ab-

sorption. They will be accounted for in the cases of optically thick plasmas.

Configuration interaction—i.e., the mixing between non-relativistic configurations—has not been included in the calculations, although it may induce large changes in some spectral features [33,34]. Actually, the mixing between configurations belonging to different SC's of an ion could be called a superconfiguration interaction and might be computed as such.

For the extension of the model to other fields, an essential improvement will be the replacement of the time-consuming calculation of the coefficients of the equations by an analytic method. This work is in progress. In this way, an extension to non-LTE time-dependent calculations will be made possible.

## APPENDIX: LINEARIZATION IN THE MASTER EQUATION

In the master equation, the fraction

$$\frac{\alpha(P,SC'\rightarrow SC)+\beta(P,SC'\rightarrow SC)\Delta E(C_i)}{\Sigma_{P,SC'}[\gamma(P,SC'\rightarrow SC)+\delta(P,SC'\rightarrow SC)\Delta E(C_i)]} \tag{A1}$$

is not, *a priori*, a linear function of $\Delta E(C_i)$. In general, it can be approximated by the nonlinear function $\lambda + \mu \exp[\varepsilon \Delta E(C_i)]$. Three appropriate values of $\Delta E(C_i)$ are chosen for computing the constants $\lambda$, $\mu$, and $\varepsilon$. These values are $\Delta E(C_0)/3$, 0, and $-\Delta E(C_0)/3$, where $C_0$ is the ground configuration of $SC$ [$\Delta E(C_0)<0$]. They correspond to the energy range of $SC$ where the configuration distribution is the most dense. By identifying the fraction with the nonlinear function, three equations are obtained. For example, the equation with $\Delta E(C_i)=0$ yields

$$\lambda + \mu = \frac{\alpha(P,SC'\rightarrow SC)}{\Sigma_{P,SC'}\gamma(P,SC\rightarrow SC')}. \tag{A2}$$

The other two equations yield, *in fine*,

$$\varepsilon = \frac{3}{\Delta E(C_0)}\ln\left(\frac{\Sigma_{P,SC'}[\gamma(P,SC\rightarrow SC')-\delta(P,SC\rightarrow SC')\Delta E(C_0)/3]}{\Sigma_{P,SC'}[\gamma(P,SC\rightarrow SC')+\delta(P,SC\rightarrow SC')\Delta E(C_0)/3]}\right) \tag{A3}$$

and

$$\mu = \frac{\Delta E(C_0)}{3\{\exp[\varepsilon\Delta E(C_0)/3]-1\}}\frac{[\beta(P,SC'\rightarrow SC)\Sigma_{P,SC'}\gamma(P,SC\rightarrow SC')]-[\alpha(P,SC'\rightarrow SC)\Sigma_{P,SC'}\delta(P,SC'\rightarrow SC)]}{[\Sigma_{P,SC'}\gamma(P,SC\rightarrow SC')+\delta(P,SC\rightarrow SC')\Delta E(C_0)/3][\Sigma_{P,SC'}\gamma(P,SC\rightarrow SC')]}. \tag{A4}$$

By expanding linearly the function $\exp[\varepsilon\Delta E(C_i)]$, one finds that the coefficients $q(P,SC'\rightarrow SC)$ and $r(P,SC'\rightarrow SC)$ in Eqs. (10)–(12) are equal to $(\lambda + \mu)$ and $\mu\varepsilon$, respectively.

[1] P. Audebert, R. Shepherd, K. B. Fournier, O. Peyrusse, D. Price, R. Lee, P. Springer, J.-C. Gauthier, and L. Klein, Phys. Rev. Lett. **89**, 265001 (2002).

[2] S. B. Hansen, A. S. Shlyaptseva, A. Y. Faenov, I. Y. Skobelev, A. I. Magunov, T. A. Pikuz, F. Blasco, F. Dorchies, C. Stenz, F. Salin, T. Auguste, S. Dobosz, P. Monot, P. D'Oliveira, S. Hulin, U. I. Safronova, and K. B. Fournier, Phys. Rev. E **66**, 046412 (2002).

[3] C. Chenais-Popovics, V. Malka, J.-C. Gauthier, S. Gary, O. Peyrusse, M. Rabec-LeGloahec, I. Matsushima, C. Bauche-Arnoult, A. Bachelier, and J. Bauche, Phys. Rev. E **65**, 046418 (2002).

[4] M. E. Foord, S. H. Glenzer, R. S. Thoe, K. L. Wong, K. B. Fournier, B. G. Wilson, and P. T. Springer, Phys. Rev. Lett. **85**, 992 (2000).

[5] M. Tabak, J. Hammer, M. E. Glinsky, W. L. Kruer, S. C. Wilks, J. Woodworth, E. M. Campbell, M. D. Perry, and R. J. Mason, Phys. Plasmas **1**, 1626 (1994).

[6] A. S. Shlyaptseva, S. B. Hansen, V. L. Kantsyrev, D. A. Fedin, N. Ouart, K. B. Fournier, and U. I. Safronova, Phys. Rev. E **67**, 026409 (2003).

[7] K. L. Wong, P. T. Springer, J. H. Hammer, C. A. Iglesias, A. L. Osterheld, M. E. Foord, H. C. Bruns, J. A. Emig, and C. Deeney, Phys. Rev. Lett. **80**, 2334 (1998).

[8] S. H. Glenzer, K. B. Fournier, B. G. Wilson, W. Lee, and L. J. Suter, Phys. Rev. Lett. **87**, 045002 (2001).

[9] P. V. Nickles, V. N. Shlyaptsev, M. Kalachnikov, M. Schnürer, I. Will, and W. Sandner, Phys. Rev. Lett. **78**, 2748 (1997).

[10] R. W. Lee, J. K. Nash, and Y. Ralchenko, J. Quant. Spectrosc. Radiat. Transf. **58**, 737 (1997).

[11] D. R. Bates, A. E. Kingston, and R. W. P. McWhirter, Proc. R. Soc. London, Ser. A **267**, 297 (1962).

[12] R. W. P. McWhirter, Phys. Rep. **37**, 165 (1978).

[13] O. Peyrusse, J. Phys. B **32**, 683 (1999).

[14] A. Bar-Shalom, J. Oreg, W. H. Goldstein, D. Shvarts, and A. Zigler, Phys. Rev. A **40**, 3183 (1989).

[15] O. Peyrusse, J. Phys. B **33**, 4303 (2000); J. Quant. Spectrosc. Radiat. Transf. **71**, 571 (2001).

[16] D. Layzer, Ann. Phys. (N.Y.) **8**, 271 (1959).

[17] A. Bar-Shalom, J. Oreg, and M. Klapisch, Phys. Rev. E **56**, R70 (1997); J. Quant. Spectrosc. Radiat. Transf. **65**, 43 (2000).

[18] M. Busquet, Phys. Fluids B **5**, 4191 (1993); M. Klapisch and A. Bar-Shalom, J. Quant. Spectrosc. Radiat. Transf. **58**, 687 (1997).

[19] J. Bauche, C. Bauche-Arnoult, and M. Klapisch, Adv. At. Mol. Phys. **23**, 131 (1987).

[20] G. Racah, Phys. Rev. **62**, 438 (1942); **76**, 1352 (1949).

[21] B. R. Judd, *Operator Techniques in Atomic Spectroscopy* (McGraw-Hill, New York, 1963).

[22] C. Bauche-Arnoult, J. Bauche, and J. O. Ekberg, J. Phys. B **15**, 701 (1982).

[23] H. Van Regemorter, Astrophys. J. **136**, 906 (1962).

[24] J. Bauche and C. Bauche-Arnoult, J. Phys. B **33**, L283 (2000).

[25] K. B. Fournier, J. Bauche, and C. Bauche-Arnoult, J. Phys. B **33**, 4891 (2000).

[26] A. Bar-Shalom, M. Klapisch, and J. Oreg, J. Quant. Spectrosc. Radiat. Transf. **71**, 169 (2001).

[27] M. Busquet and P. Cossé, J. Quant. Spectrosc. Radiat. Transf. **65**, 101 (2000); and private communication.

[28] C. Bauche-Arnoult and J. Bauche, J. Quant. Spectrosc. Radiat. Transf. **71**, 189 (2001).

[29] J. Bauche, C. Bauche-Arnoult, E. Luc-Koenig, J.-F. Wyart, and M. Klapisch, Phys. Rev. A **28**, 829 (1983).

[30] J. Bauche and C. Bauche-Arnoult, in *Laser Interactions with Atoms, Solids and Plasmas*, edited by R. M. More (Plenum Press, New York, 1994).

[31] J. Bauche, C. Bauche-Arnoult, O. Peyrusse, A. Bachelier, K. B. Fournier, C. Chenais-Popovics, and J.-C. Gauthier, J. Quant. Spectrosc. Radiat. Transf. **81**, 47 (2003).

[32] J. R. Albritton and B. G. Wilson, Phys. Rev. Lett. **83**, 1594 (1999).

[33] J. Bauche, C. Bauche-Arnoult, M. Klapisch, P. Mandelbaum, and J.-L. Schwob, J. Phys. B **20**, 1443 (1987).

[34] J. Bauche and C. Bauche-Arnoult, J. Phys. B **22**, 2503 (1989).